Zeolite 4A Coating by Polypyrrole Doped with Chlorine

FAHIM HAMIDOUCHE, NACER EDDINE DJELALI*, ZOHRA GHABACHE
Laboratory of processing and formatting of polymers LTMFP, University M'hamed Bougara, Boumerdes - UMBB -Algeria.

An organic–inorganic conductor's Polypyrrole(Cl)/Zeolite 4A (PPy(Cl)/Z4A) was successfully synthesized by chemical oxidative polymerization at low and room temperature, using $FeCl_3$ as initiator the reaction and dopant at the same time. After characterization, commodity we methods primarily on the polymerization of pyrrole with different molar ratios of [$FeCl_3$]/[Pyrrole] in an aqueous medium, followed by a series of characterizations for the polymers obtained. The right ratio was used for the preparation of nanocomposites PPy(Cl)/Z4A. After each synthesis, the developed product is characterized by FTIR, SEM-EDX, XRD, electrical conductivity and cyclic voltammetry, in order to confirm the success of the process of synthesis and study their properties to specific applications envisaged.

Keywords: Nonocomposite, Polypyrrole, Zeolite 4A, Conductor Polymer

Polypyrrole (PPy) is the first commercially available conductive polymer due to its good stability in air and heat, as well as its low cost with potential applications such as electromagnetic shielding, capacitors, sensors, antistatic packaging, anti-corrosion coating, etc. In general, Polypyrrole has a good specific capacity, but a low cyclic stability, there have been several attempts to improve the cyclic stability of PPy by mixing with polymers and additives such as silica fume and insulation zeolites.

Zeolites are materials that have fascinated man since their discovery by A. F. Cronsted. Due to speciûc pore size and large surface area, these materials have success in molecular sieves, adsorbents, catalysts, electrodes and micro fuel cells…etc. Zeolites could be divided into various kinds according to their structural characteristics, such as A, X, Y, ZSM-5, and mordenite. Among them, single phase Z4A has been of great interest for its highest cation exchange capacity and largest number of acidity sites, which is widely used in adsorption and ion exchange processes such as drying gases and liquids, washing builder and separation of normal from branched parafuns [1].

The Z4A was the subject of our study, that is a synthetic aluminosilicate having a chemical composition of $Mx/n[(AlO_2)x(SiO_2)y].zH_2O$ (M = exchangeable cation, especially alkali or alkaline n= valence of cation), with a defined, micro-pores of uniform network [2].

The work presented in this manuscript is to explore other avenues for the synthesis of nanocomposites based conductive polypyrrole as a template, the Zeolite 4A as reinforcements with the optimization of operating conditions in order to increase the value of the electrical conductivity.

Experimental part

Materials and methods

Characterizations of Z4A

a)XRF analysis

Chemical analysis of the Z4A shows that the main components of the zeolite present in the structure were determined [3].

b)X-ray diffraction analysis

Figure 1 shows diagrams of the Z4A. The high intensity peaks indicated that the products presented high crystallinity [4]. No peaks other impurities were detected in the two modes, which indicates that only the phase of Z4A which are in the sample [1, 5].

The Scherrer method was used to calculate the mean particle size that is expressed by the following formula:

$$D_{Scherrer} = \frac{k\lambda}{\beta \cos\theta} \quad (1)$$

W\where λ is the wavelength of the X-ray radiation (λ = 0.154056 nm), K is the Scherrer constant (k = 0.89), θ is the diffraction angle and β is the line width at half-maximum height of the most intense peak.

The average crystallite sizes of each sample calculated by Scherrer formula [6] are shown in the following table 1.

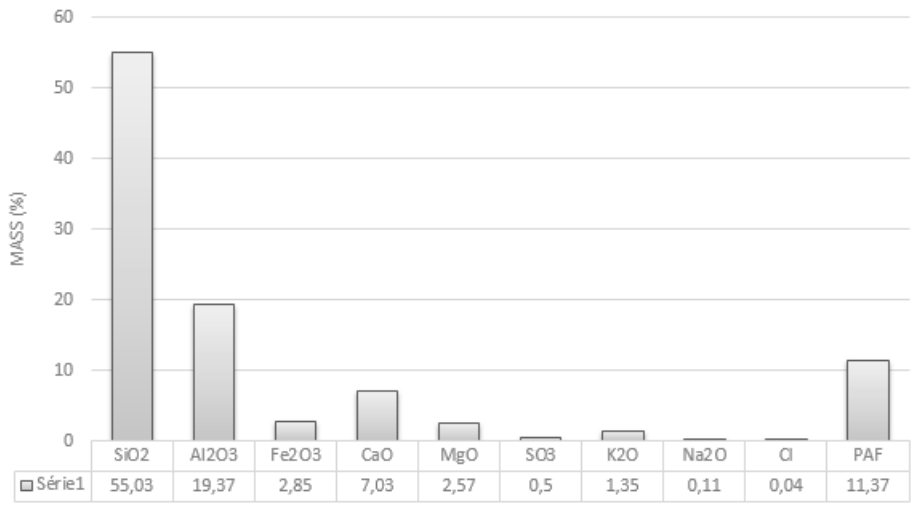

Fig. 1. Chemical composition of Z4A

* email: djelnac@yahoo.fr

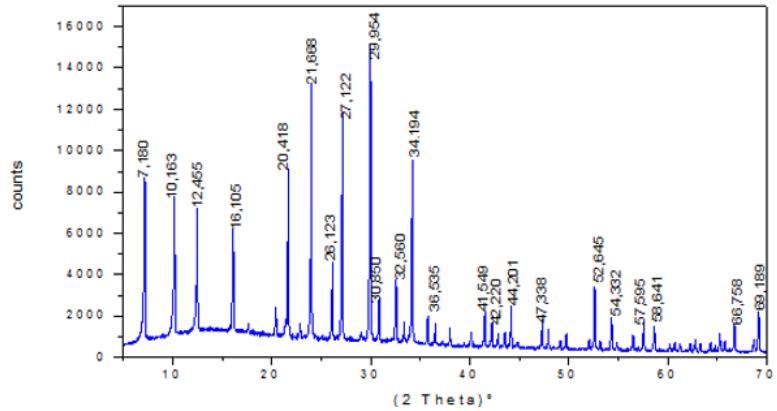

Fig. 2. Overlay XRD for Z4A

Martial	2θ	d[A]	Miller Indices			β	$D_{Scherrer}$ (nm)
			h	k	l		
Z4A	29,981	2,978	4	1	0	0,081	1,731

Table I
CRYSTALLITE SIZE OF THE Z4A

c)SEM and EDX analysis

The presence of irregular particles on the surface of zeolite or between the particles was observed in inset micrograph (fig. 3a) [7]. The EDX mapping and XRF analysis (fig. 3b) reveals that the main chemical compositions of zeolite include Na, Al, Si, and Fe. The further EDX and XRF analysis also show the chemical compositions of chamfered-edged cubes include Si, Al, Na and Fe [1].

d) Particle size distribution

Z4A is supplied as a powder, with an average particles size of approximately 3 microns. The narrow particle size distribution figure 4 ensures proper application of Z4A in specific areas [8].

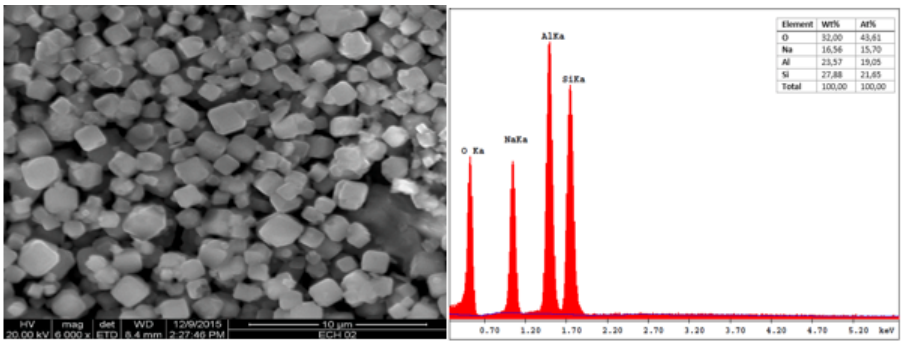

Fig. 3. SEM micrograph (a) and EDX spectrum (b) of the Z4A

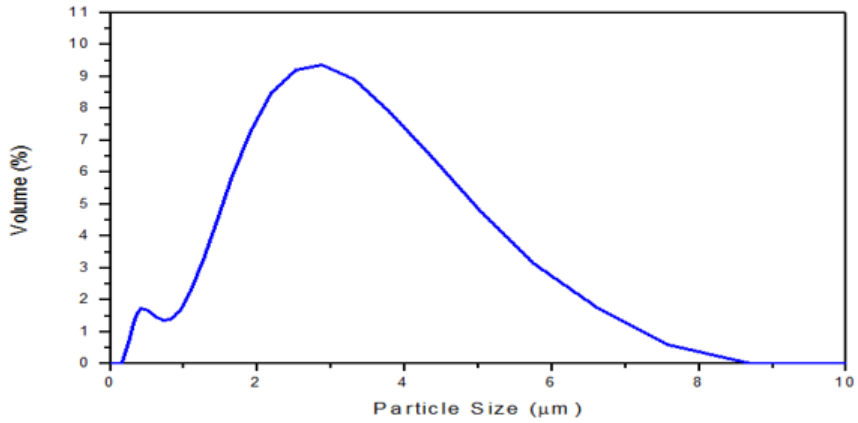

Fig. 4. Average particles size of the Z4A.

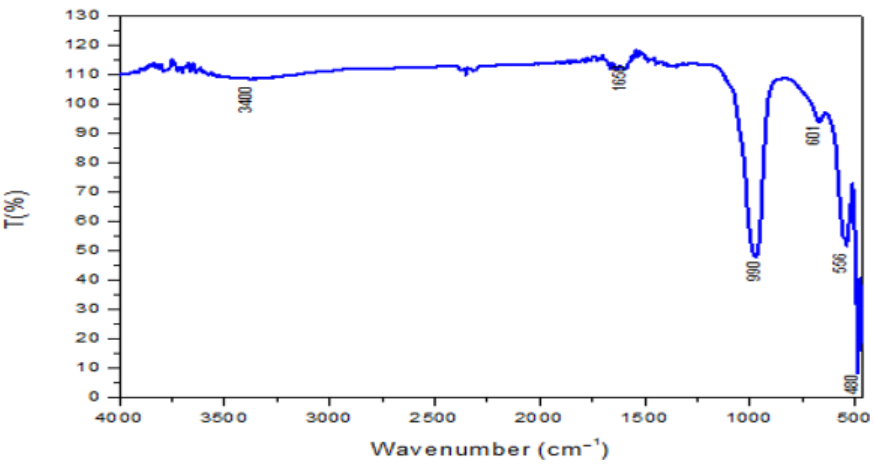

Fig. 5. FTIR spectrum of Z4A

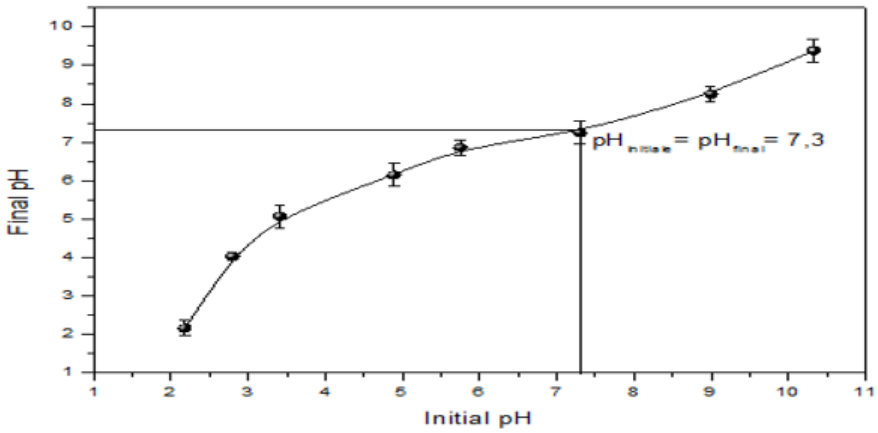

Fig. 6. *p*H of the point zero charge pHpzc of the Z4A.

e) FTIR analysis

The FTIR spectrum of the Z4A is shown in figure 5 In the spectrum, all of the adsorption bands related to zeolite were observed. The bands at 465, 560 and 601 cm^{-1} are assigned to the vibrations of T-O bending, the double ring bending, and the TO_4 asymmetric stretch (T ¼ Si or Al), respectively. The band at 3000-3600 cm^{-1} represents the intra- and inter-molecular hydrogen bonding, and the band at 1650 cm^{-1} is related to interstitial bonded water [1,9].

f) Determination of zero point charge *p*H(zpc)

The isoelectric *p*H $pH_{(zpc)}$ corresponds to the point where the total charge of the Z4A zero. It is determined according to the *Cerovic* method [1], by the shape of the curve $pH_{final} = f(pH_{initial})$. $pH_{(zpc)}$ represents the point where the curve is equal to the $pH_{final} = pH_{initial}$. The $pH_{(zpc)}$ of the Z4A is 7.3, it is deducted graphically in figure 6 [10].

Materials synthesis

In a 100 mL flask, we have prepared a solution based Z4A in 50 mL of distilled water (with a report of mass [Z4A]/[Pyrrole] = 0.1 - 0.2 - 0.3 - 0.4 - 0.5) under stirring for one hour. We then added 1.4 mL of pyrrole ($pH_{(zpc)}$ = 5.56) [11], under agitation also during 4h at *p*H between 6-7. We see the emergence of a creamy solution in both cases. The polymerization in room temperatures and of 0°C is initiated by the injection drop wise 50 mL of a solution of oxidizing $FeCl_3$ (using the best molar ratio ([$FeCl_3$]/[Pyrrole]=2.5) obtained according to the results of characterizations of PPy(Cl)). After 3h of polymerization, the nanocomposites obtained were filtered, washed completely with water to remove the oxidant and the traces of pyrrole not reacted, then with methanol to remove the remaining oligomers. Finally, the nanocomposites obtained are made dry in an oven between 60 to 70°C for eight hours.

Characterizations

FTIR spectra analysis

We observe at 1665, 980, 661, 560 and 495 cm^{-1} the appearance of vibration bands of Z4A (8). In contrast, bands which appear at 1540, 1434, 1280, 1130, 1020, 980, 850 and 740 cm^{-1} is the vibrations of PPy(Cl) (12; 13; 14). This means that the Z4A channels in our case the PPy(Cl). In suggesting this, the zeolite is involved only to compensate the positive charge on PPy(Cl).

The main infrared vibrational bands for identifying PPy(Cl) and Z4A were observed, confirming the good progress of the polymerization process.

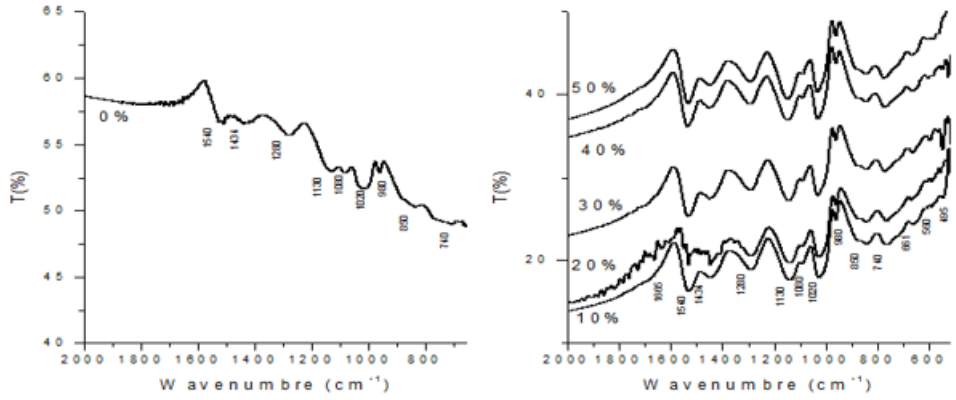

Fig. 7. Overlay of infrared spectra of the nanocomposites synthesis with the report [$FeCl_3$]/[Pyrrole] = 2.5, T = 0°C and different mass percentages of the Z4A

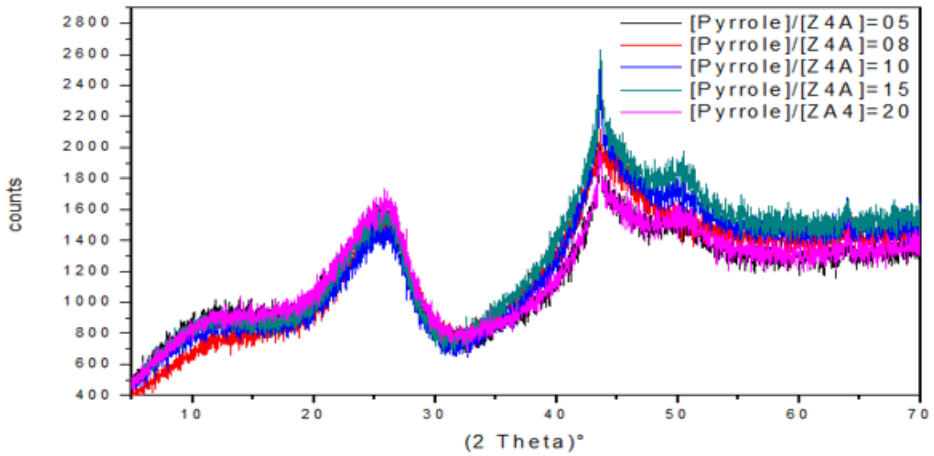

Fig. 8. Superposition of spectral XRD of nanocomposites synthesis with the report [$FeCl_3$]/[Pyrrole] = 2.5 and different weight percentages of the Z4A.

X-ray diffraction (XRD) analysis

The results obtained by X-ray diffraction (XRD) performed on the powders of PPy(Cl)/Z4A have enabled us to conclude that they are of amorphous structures [15], therefore the Z4A is fully coated by the PPy(Cl).

There is an interaction between the Z4A and the pyrrole, which reveals a superficial adsorption limited leading to a polymerization in-situ which has as result, PPy(Cl) hooked to the pores, therefore the formation of envelope by the PPy(Cl) on the Z4A. The following figure illustrates a proposal of mechanism for the polymerization of pyrrole on the surface of the Z4A.

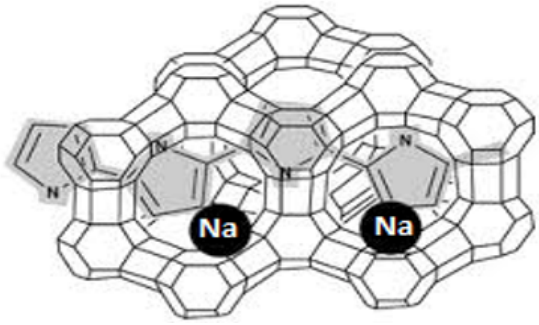

Fig. 9. Polymerization of Pyrrole on the surface of the Z4A.

Measurement of the electrical conductivity by four-probe method

Applying a pressure on four points spaced by a distance of the sample surface allowed us give a precise resistivity measured in samples having different shapes, which can be expressed by the following formula:

$$\varphi = \frac{\varphi_\circ}{G_7(W/S)}\ (\Omega.cm) \qquad (2)$$

$$\varphi_\circ = \frac{V}{I} 2\pi S \qquad (3)$$

$$G_7(W/S) = \frac{2S}{W} ln\, 2 \qquad (4)$$

Where φ is an electrical resistivity with the correction coefficient, **S** is a distance between the centers (s) = 2.0 mm, W is a thickness of the wafer and $\varphi_\circ$ is an electrical resistivity without correction coefficient [16].

The nanocomposites based semiconductors of PPy(Cl)/Z4A, as can be seen on the figure 8, although the PPy(Cl) is amorphous, the structure of the cavities of the 4A zeolite improves the alignment of the chains of PPy(Cl) by the adsorption of the latter on the surface of the grain, which increase the conductivity mounting and coasts the aging.

The electrical conductivity increases with increasing mass ratio [Z4A]/[Pyrrole] up to a ratio of 0.3 with δ = 6.61 S/cm (17). Then, there is a decrease in the presence of PPy(Cl) saturation phenomenon with the particles Z4A.

Analysis by Scanning electron microscope (SEM)

According to the micrographs, below, there is a marked evolution of the morphology of nanocomposites conductors in function of the rate of Z4A incorporated.The particles of the Z4A are covered by the PPy(Cl) with a spherical nature dispersed in the polymeric matrix, forming clumps of different distributions with significant proportions [18].

The optical properties (diffuse reflectance spectra)

The optical properties of the hetero-system [$FeCl_3$]/[Pyrrole] = 2.5 and 30 % wt of Z4Adetermined by the diffuse reflectance spectra. The relation between the absorption coefficient (α) and incident photon energy (hμ) is given by the Tauc relation:

$$(\alpha h\mu)^m = C(h\mu - E_g) \qquad (5)$$

C is a constant, the exponent m depends on the transition type, m=2 and 1/2 respectively for direct or indirect transitions. The intercept of the linear plot $(\alpha h\mu)^2$ of the heterosystem with the $h\mu$ -axis figure 12 yield direct optical transition at 1.129 eV [19].

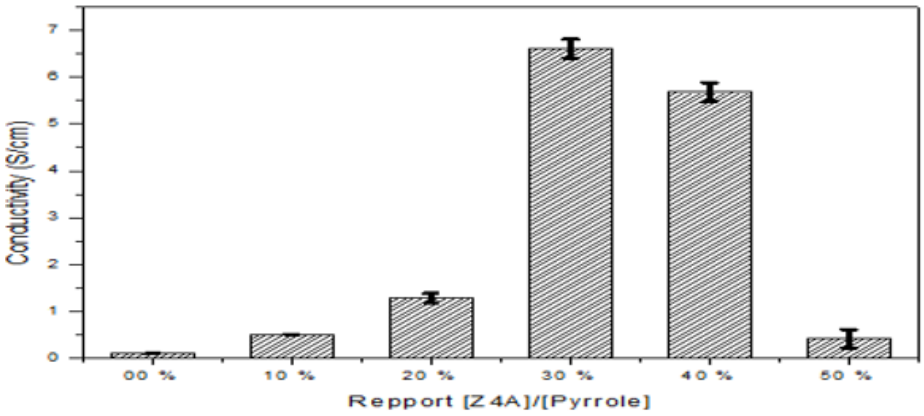

Fig. 10. Evolution of the electrical conductivity of the nanocomposites synthesis with the report [$FeCl_3$] / [Pyrrole] = 2.5, T = 0°C and different mass percentages of the Z4A.

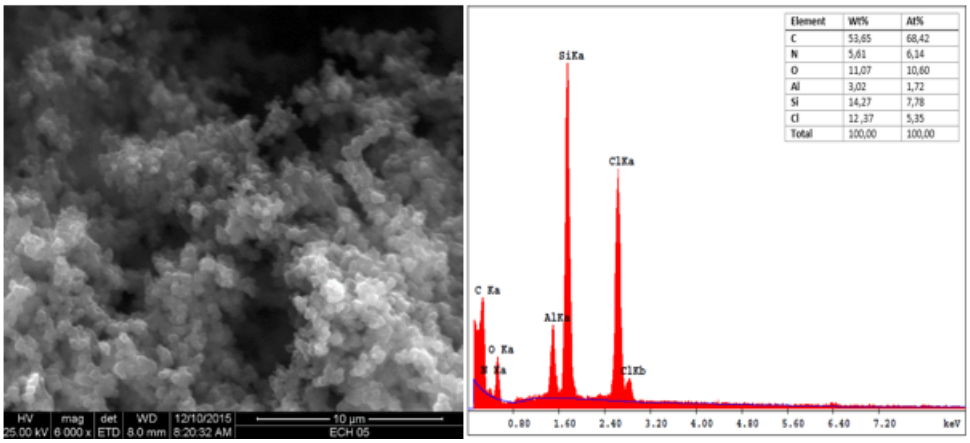

Fig. 11. SEM micrograph (a) and EDX spectrum (b) of nanocomposite based PPy(Cl)/ 30% Z4A (synthesized at T= 0°C)

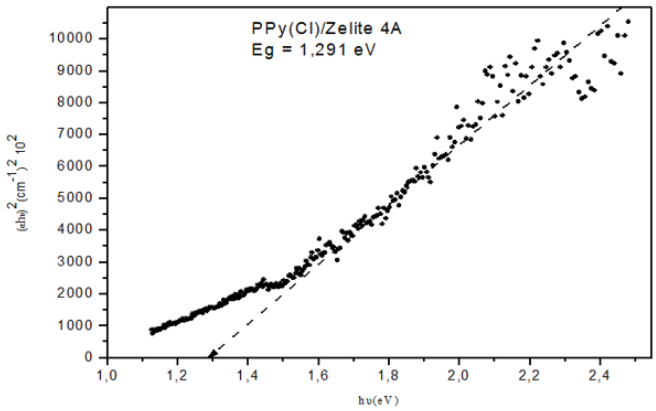

Fig. 12. The direct optical transitions of nanocomposite based PPy(Cl)/30% Z4A (synthesized at T= 0°C)

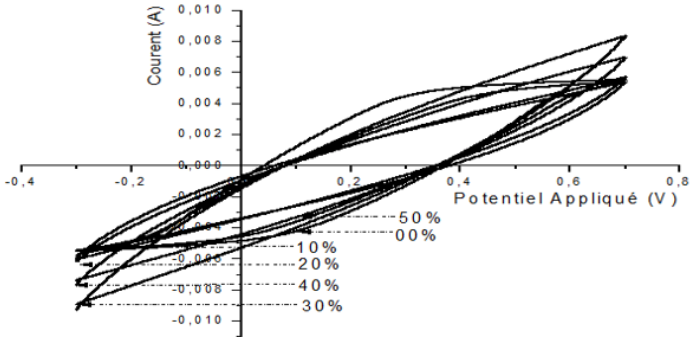

Fig. 14. Overlay of the cyclic voltammograms at 20 mV/s of the nanocomposites synthesis with report [$FeCl_3$] / [Pyrrole] = 2.5, T = 0°C and different mass percentages of the Z4A, showing the stability of potential window with 1 mol . L-1 H_2SO_4 electrolyte

Electrochemical measurements

In this part, we will study the influence of chemical synthesis conditions nanocomposites polypyrrole (temperature, duration and type of oxidant) on its electrochemical reactivity in the aqueous medium H_2SO_4 1 mol L^{-1}. The reactivity of these powders will be considered by cyclic voltammetry, by introducing a small amount of the synthesized powder, about 3 to 6 milligrams.

The experiments were performed in an electrochemical cell with three electrodes, namely a reference electrode (Ag/AgCl), a platinum gate (against electrode) and the working electrode. The cyclic voltammetry measurements were performed in the potential range from -0.3 to 0.7V Ag/AgCl, starting with a scanning cathode potential.

a) Electrochemical stability domain of electrolytes

After several steps, before we choose the potential window of between -0.3 and 0.7 V which is close to the ideal voltamperogram rectangular shape of a supercapacitor.

b) Influence of mass ratio [Z4A]/[Pyrrole]

We note that the surface of the voltammogram increases with increase in the percentage of Z4A in the PPy matrix to weight ratio of 30%, which reflects an increase in specific capacity of the electrode. A decrease in the surface of voltamperogram from the percentage 40% is observed. These results are in perfect agreement with the results of the conductivity, which we bring to say that an improvement in conductivity causes the increase in specific capacity and therefore improving performance nanocomposite.

The figure shows a marked improvement in the poypyrrole specific capacity in the presence of the particles

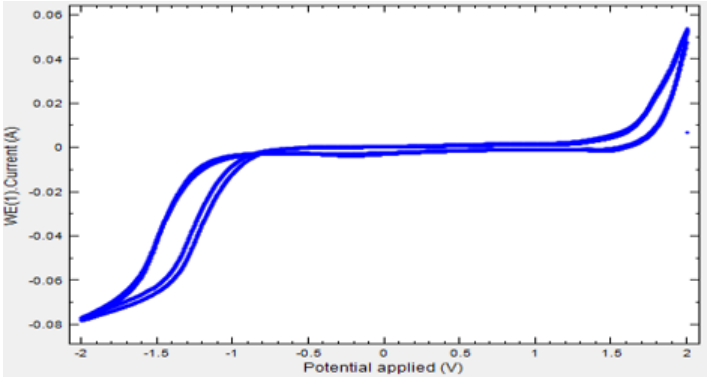

Fig. 13. Cyclic voltammogram at 10 mV/s showing the stability of potential window of the electrolyte H_2SO_4 1mol.L^{-1}

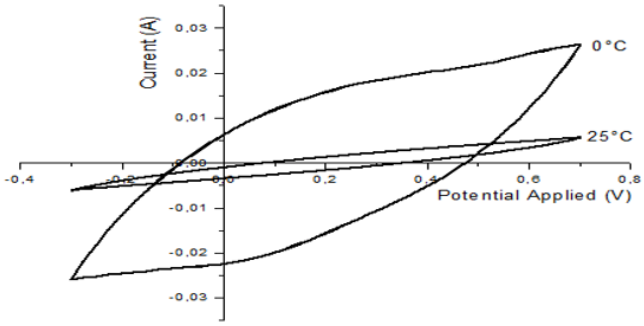

Fig. 15. Second comparison cycle voltammogram at speed of 20 mV/s for nanocomposites based PPy(Cl) / 30% Z4A synthesized at 0 and 25 ° C

at 30% by weight of Z4A, which gives a slight improvement in the stability of the nanocomposite relative to the pure polymer.

c)Influence of the scanning speed of nanocomposites PPy(Cl)/ 30% Z4A

The following figure shows the cyclic voltammograms (CV) of nanocomposite based PPy(Cl)/Z4A with a percentage of 30% at different scan speeds ranging from 200 to 5 mV/s in 1 mol L^{-1} H_2SO_4.

As speed increases, the oxidation and reduction peaks in figure narrowed to and increases toward the positive and negative potential, respectively, which could be attributed to a resistance increase, which may originate from the good conductivity electronic of material.

The influence of the scanning velocity on the specific capacitance is observed. The highest values of specific capacitance are always obtained by using higher sampling rates [20].

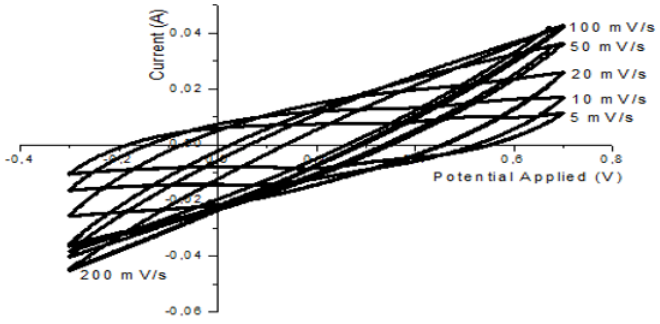

Fig. 16. Cyclic voltammograms (CV) of nanocomposite based PPy(Cl)/ 30% Z4A (synthesized at T= 0°C) with different scanning speeds ranging from 200 to 5 mV/s in H_2SO_4 1 mol.L^{-1} as supporting electrolyte

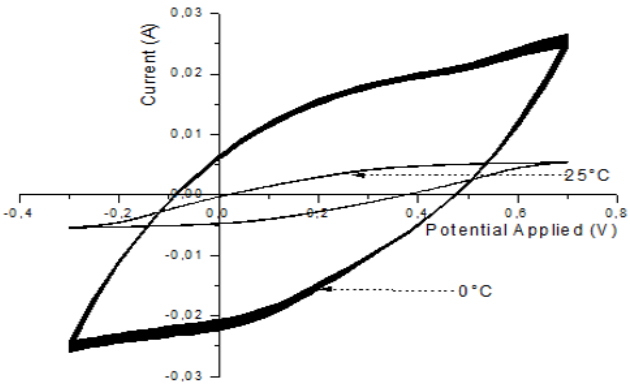

Fig. 17. Cyclic voltammograms of 100 cycles at 20 mV/s of nanocomposite based PPy(Cl)/ 30% Z4A synthesized at T = 0°C and 25°C, H_2SO_4 1 mol.L^{-1} as supporting electrolyte

d) Stability study at the 100 cycles

The study at the cyclic stability nanocomposite based PPy(Cl)/30% Z4A was carried out at 20 mV/s for 100 cycles and the results are presented in figure 17.

Conclusions

The work done in this manuscript the exploration of the ways that facilitate the synthesis of nanocomposites drivers with mineral heart (Z4A) covered with an envelope of PPy(Cl), which allowed us to understand the relationship between texture nanocomposites (via interactions between the polymer chains and reinforcements) and the carrier mobility (fundamental parameter for organic electronics applications) to improve their electrical properties for specific applications.

This work shows the importance of the diversity of characterizations for the study of these materials, a performance analysis protocol was developed with the choice of evaluation parameters (FTIR, Electrical Conductivity (S/cm) SEM-EDX, XRD).

All work met the goals we set at the beginning that the Z4A are completely coated by PPy(Cl) with the improved alignment of the latter channels that allow increased conductivity electric.

Finally, this study will enable better management of nanocomposites based drivers of PPy(Cl) with the incorporation of the Z4A, and opening up a new route for the design of specific applications, and the results will form the basis the techno-economic calculation for possible exploitation

References

1. XIAOMIN NI. and al., Fabrication of hierarchical zeolite 4A microspheres with improved adsorption capacity to bromo-fluoropropene and their fire suppression performance, Journal of Alloys and Compounds , Vol. 592 , pp. 135–139, 2014.
2. PETER MULLER, ALEXANDER RUSSELL, JURGEN TOMAS, Influence of binder and moisture content on the strength of zeolite 4A granules, Chemical Engineering Science, Vol. 126, pp. 204–215, 2015.
3. JALIL R. UGAL, KARIM H. HASSAN AND INAM H. ALI. Preparation of type 4A zeolite from Iraqi kaolin, Journal of the Association of Arab Universities for Basic and Applied Sciences, Vol. 9, pp. 2-5, 2010.
4. TUYEN L. A. and al., Structural effects induced by 2.5 MeV proton beam on zeolite 4A: Positron annihilation and X-ray diffraction study. Radiation Physics and Chemistry, Vol. 06, pp. 355–359, 2015.
5. MAHFOUD BARKAT and al., Uranium (VI) adsorption on synthesized 4A and P1 zeolites: Equilibrium, kinetic, and thermodynamic studies, C. R. Chim., 18, pp. 261–269, 2015.
6. ALLEN W. BURTON and al., On the estimation of average crystallite size of zeolites from the Scherrer equation: A critical evaluation of its application to zeolites with one-dimensional pore systems, Microporous and Mesoporous Materials, Vol. 117, pp. 75–90, 2009.
7. DONGYANG MA. and al., Feasible conversion of solid waste bauxite tailings into highly crystalline 4A zeolite with valuable application, Waste Management, Vol. 34, pp. 2365–2372, 2014.
8. WEIQING WANG and al.,novel magnetic 4A zeolite adsorbent synthesised from kaolinite type pyrite cinder (KTPC), Solid State Sciences , Vol. 39 , pp. 52-58, 2015.
9. MERVE BICEN and al., The effect of surface modification of zeolite 4A on the physical and electrical properties of copolyimide hybrid films, Microporous and Mesoporous Materials, Vol. 218, pp. 79-87, 2015
10. CEROVIC LJ. S. and al., Point of zero charge of different carbides, Physicochemistry Enginneering Aspects, Vol. 297, pp. 1-6, 2007.
11. HUI QI, and al., Synthesis of an organic–inorganic polypyrrole/titanium(IV) biphosphate hybrid for Cr(VI) removal, Journal of Molecular Liquids, Vol. 215, pp. 402–409, 2016.
12. RADHAKRISHNAN S., Santhosh Paul, Conducting polypyrrole modified with ferrocene for applications incarbon monoxide sensors, Sensors and Actuators, Vol. B 125, pp. 60-65, 2007.
13. XIN TUO and al., Facile assembly of polypyrrole/Prussian blue aerogels for hydrogen peroxide reduction. Synthetic Metals, Vol. 213, pp. 73–77, 2016.
14.ZOHREH DELJOO KOJABAD, SEYED ABBAS SHOJAOSADATI, Chemical synthesis of polypyrrole nanostructures: Optimization and applications for neural microelectrodes, Materials and Design , Vol. 96, pp. 378–384, 2016.
15.VISHNUVARDHAN T. K. and al., Synthesis, characterization and a.c. conductivity of polypyrrole/Y_2O_3 Composites. al., Indian Academy of Sciences, Vol. 29, pp. 77–83, 2006.
16. AIHUA CHEN and al., Influence of concentration of $FeCl_3$ solution on properties of polypyrrole–Fe_3O_4 composites prepared by common ion absorption effect, Synthetic Metals, Vol. 145, pp. 153–157, 2004.
17. JANA TABACIAROVA and al., Study of polypyrrole aging by XPS, FTIR and conductivity measurements, Polymer Degradation and Stability, Vol. 120, pp. 392-401, 2015.
18. HEMANT K. CHITTE and al.,Synthesis of Polypyrrole Using Ferric Chloride ($FeCl_3$) as Oxidant Together with Some Dopants for Use in Gas Sensors, Journal of Sensor Technology, Vol. 1, pp. 47-56, 2011.
19. BELABED C. and al., Photocatalytic hydrogen evolution on the hetero-system polypyrrol/TiO2 under visible light. international journal o f hydrogen energy, Vol. 17, pp. 533-539, 2014.
20. PUSHPENDRA K. SHARMA and al., Synthesis and characterization of polypyrrole by cyclic voltammetry at different scan rate and its use in electrochemical reduction of the simulant of nerve agents , Synthetic Metals, Vol. 160, pp. 2631–2637, 2010.
21.VITORATOS E., Conductivity and thermal aging of conducting Zeolite/Polyaniline and Zeolite/Polypyrrole blends, Current Applied Physics Vol. 7, pp. 578–581, 2007.

Manuscript received: 14.12.2015